Electronic Supplementary Material (ESI) for Faraday Discussions.
This journal is © The Royal Society of Chemistry 2018

Supporting Information

DFT calculation of oxygen adsorption on platinum nanoparticles: Coverage and size effects

L.G. Verga,[a] J. Aarons,[a] M. Sarwar,[b] D. Thompsett,[b] A.E. Russell,[a] and C-K. Skylaris[a*]

[a] Department of Chemistry, University of Southampton, Highfield, Southampton SO17 1BJ, United Kingdom

[b] Johnson Matthey Technology Centre, Blounts Court, Reading, Berkshire, UK RG4 9NH

E-mail:[*] *c.skylaris@soton.ac.uk*

1 Coulomb-cutoff radius

We performed our calculations with the spherical Coulomb-cutoff to avoid any interaction between the system and the periodic images. We defined the minimum Coulomb-cutoff radius r_{CC} after a convergence test with O adsorption at a hollow site in a (111) facet of a cuboctahedral Pt_{55} nanoparticle with a diameter of approximately 11 Å. The following table shows how the adsorption energy changes with the Coulomb-cutoff radius.

Table 1 Oxygen adsorption energies for different values of coulomb-cutoff radius.

r_{CC} (Å)	E_{ADS} (eV)
12	-11.68
22	-0.89
32	-0.88
36	-0.88
44	-0.88

The first r_{CC} value is larger than the maximum inter-atomic distance inside our system $rmax_{ij}$, while the second r_{CC} value includes $rmax_{ij}$ and two times the NGWF radius r_{NGWF}. We only observed fluctuations in the adsorption energies happened for r_{CC} between these limits. Thus, to ensure convergence within the Coulomb-cutoff radius, we used a minimum r_{CC} which is calculated with the following equation:

$$r_{CC} = rmax_{ij} + 2r_{NGWF} + a \tag{1}$$

where we add the maximum inter-atomic separation, two times the NGWF radius, and a constant value a of at least 5 Å to account for Gibbs oscillations, as the Cutoff Coulomb operator is computed in reciprocal space.

2 Initial and Final O distribution

As discussed in the main article, the initial O distribution with a given O coverage is different for each nanoparticle size, as the ratio between adsorption sites in the edges and vertices of the nanoparticle and terrace sites is size dependent. Figure 1 shows the initial and final O configuration for Pt_{55} with three different values of O coverage. At this nanoparticle size, we reach a 1.00ML coverage using only HCP vertex sites for (111) facets and Bridge sites near the edges for (100) facets. For 0.66ML and 1.00ML coverages, we clearly see O atoms moving from the initial HCP (111) adsorption sites to bridge sites in the vertices of the nanoparticle after the geometry optimisation.

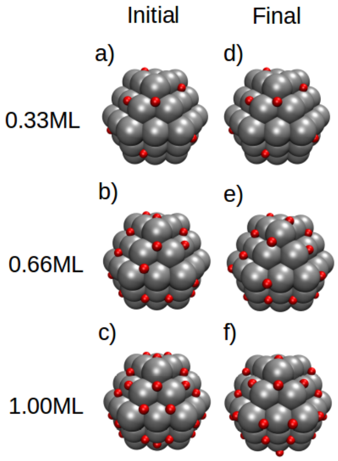

Figure 1 Pt_{55} nanoparticle covered with atomic oxygen on different coverages, where a), b), c) show initial O configuration and d), e), f) show the O configuration after geometry optimisation. Silver (red) balls represent Pt (O) atoms.

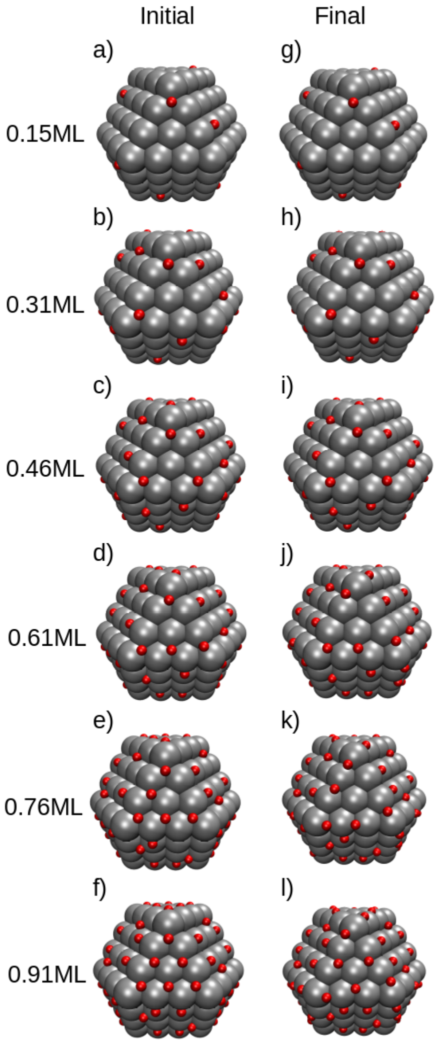

Figure 2 Pt_{147} nanoparticle covered with atomic oxygen on different coverages, where a), b), c), d) show initial O configuration and e), f), g), h) show the O configuration after geometry optimisation. Silver (red) balls represent Pt (O) atoms.

Figure 2 shows the initial and final O configuration for Pt_{147} nanoparticles with different O coverages. The O coverage up to 0.46ML is obtained by adding one O atom to a HCP vertex (111) site and one O atom to a Bridge site near the edge of (100) facet. For higher O coverages, we also use HCP edges (111) adsorption sites. Similarly to the results obtained for Pt_{55}, we only see oxygen movement between adsorption sites for systems with O coverages equal or higher than 0.60ML.

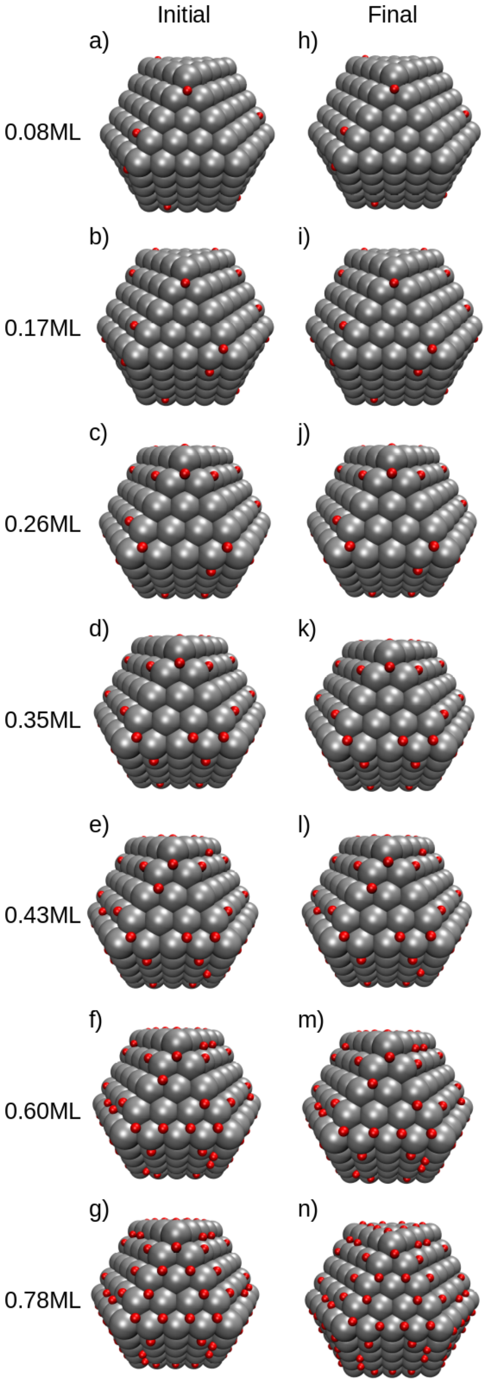

Figure 3 Pt_{309} nanoparticle covered with atomic oxygen on different coverages, where a), b), c), d), e) show initial O configuration and f), g), h), i), j) show the O configuration after geometry optimisation. Silver (red) balls represent Pt (O) atoms.

For Pt_{309} nanoparticles, as illustrated on Figure 3, we see significant changes between initial and final O configuration only for the systems with 0.78ML O coverage. For 0.6ML O coverage, we see small changes between initial and final O configurations, while for systems with lower coverage the initial and final O configuration are identical.

We calculate single O adsorption for each adsorption site present on initial or final O configurations for all nanoparticle sizes and O coverages. These values are used in the main article to calculate the average adsorption energy for the initial and final O configuration. Table 2 shows the adsorption energy for different nanoparticle sizes and adsorption sites.

Table 2 Adsorption energies for single O adsorption on different adsorption sites and nanoparticle sizes, where NE and NC are non-existent and non-computed adsorption sites.

	Pt_{55} E_{ADS} (eV)	Pt_{147} E_{ADS} (eV)	Pt_{309} E_{ADS} (eV)
HCP-V (111)	-0.87	-0.85	-0.92
HCP-E (111)	NE	-0.61	-0.69
Bridge-V (111)	-1.13	-1.00	-1.08
Bridge-E (111)	NC	-0.90	-0.90
Bridge-NE (100)	-0.85	-0.83	-0.91
Bridge-V (100)	-0.98	NC	NC
Top-E (100)	-0.36	-0.28	NC

For all the nanoparticles we examined, we see that adsorption energies for Bridge sites in the vertices and edges of the nanoparticle are comparable or stronger than those obtained for HCP sites, making easier the O movement between these two adsorption sites. For the (100) facet, the only adsorption site as strong as the initial Bridge sites located near the edge of the nanoparticle is the adsorption site in the vertex between the (100) and (111) facets. However, after geometry optimisation, the sites in the edges and vertices of the nanoparticle are occupied by O atoms moving from the HCP (111) sites. Thus, as these sites are occupied, and top sites in the edge of (100) facets are much weaker than the initial bridge sites near edge, almost no O diffusion happens for (100) facets.